# A perspective on the redox properties of tetrapyrrole macrocycles

James R. Diers,[1] Christine Kirmaier,[2] Masahiko Taniguchi,[3]

Jonathan S. Lindsey,[3] David F. Bocian,[1] and Dewey Holten[2]

[1] Department of Chemistry, University of California, Riverside, CA 92521-0403

[2] Department of Chemistry, Washington University, St. Louis, MO 63130-4889

[3] Department of Chemistry, North Carolina State University, Raleigh, NC 27695-8204

## TOC graphic

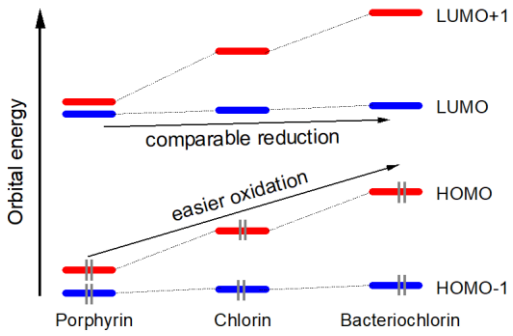

**ABSTRACT**

Tetrapyrrole macrocycles serve a multitude of roles in biological systems, including oxygen transport by heme and light harvesting and charge separation by chlorophylls and bacteriochlorophylls. Synthetic tetrapyrroles are utilized in diverse applications ranging from solar-energy conversion to photomedicine. Nevertheless, students beginning tetrapyrrole research, as well as established practitioners, are often puzzled when comparing properties of related tetrapyrroles. Questions arise as to why optical spectra of two tetrapyrroles often shift in wavelength/energy in a direction opposite to that predicted by common chemical intuition based on the size of a π-electron system. Similar, one is often puzzled as to why the oxidation potentials differ significantly when comparing two related tetrapyrroles, yet the reduction potentials change very little or shift in the opposite direction. In order to understand these properties, it is not sufficient to consider how structural alterations affect the HOMO and LUMO, but also the HOMO-1 and LUMO+1, as is the case for Gouterman's four-orbital model for tetrapyrrole optical spectra. This perspective presents a fundamental framework concerning tetrapyrrole electronic properties that should provide a foundation for rationale molecular design in tetrapyrrole science.

## INTRODUCTION

Tetrapyrrole macrocycles include porphyrins, chlorins and bacteriochlorins, which are represented by natural hemes, chlorophylls and bacteriochlorophylls, respectively, as well as diverse synthetic analogs (Figs. 1 and 2).[1] The rich optical and redox properties of tetrapyrrole macrocycles have led to their use in immensely varied applications ranging from solar-energy conversion to photomedicine (photodynamic therapy, molecular imaging, and flow cytometry). The tetrapyrrole macrocycles in such applications have been obtained by derivatization of the natural pigments (semisynthesis)[2,3] and by *de novo* synthesis, which has afforded diverse porphyrins,[4,5] chlorins,[6-8] and bacteriochlorins.[2,3,9-11] The porphyrin – chlorin – bacteriochlorin molecules constitute an homologous series with progressively decreased conjugation, respectively (Fig. 1).

Students beginning tetrapyrrole research, and even seasoned experts, often have questions regarding why the spectral and redox properties of tetrapyrroles often do not follow chemical intuition. For example, it is frequently asked how it is that even though a bacteriochlorin has overall less conjugation than its chlorin analog (Fig. 1), the longest wavelength absorption band of the bacteriochlorin is shifted to lower energy compared to that of the chlorin. Similarly, workers in the photosynthesis community often ask why the longest wavelength absorption band of Chl *b* is shifted to higher energy from that of Chl *a* even though Chl *b* has more conjugative substituents than Chl *a* (Fig. 2). These observations do not follow the logic from a particle in a box, be it linear or circular, in which the energy level spacing decreases as the size of the box increases. Along the same lines, workers often wonder why the oxidation potentials may increase markedly among a set of related tetrapyrroles yet the reduction potentials change relatively little or even shift in the opposite direction. The difficulties can be compounded when one is comparing tetrapyrroles that differ in macrocycle type (porphyrin, chlorin, or bacteriochlorin), metalation state (free base form

or metal chelate), and/or substituents (electron donating/withdrawing, conjugative, and site of substitution).

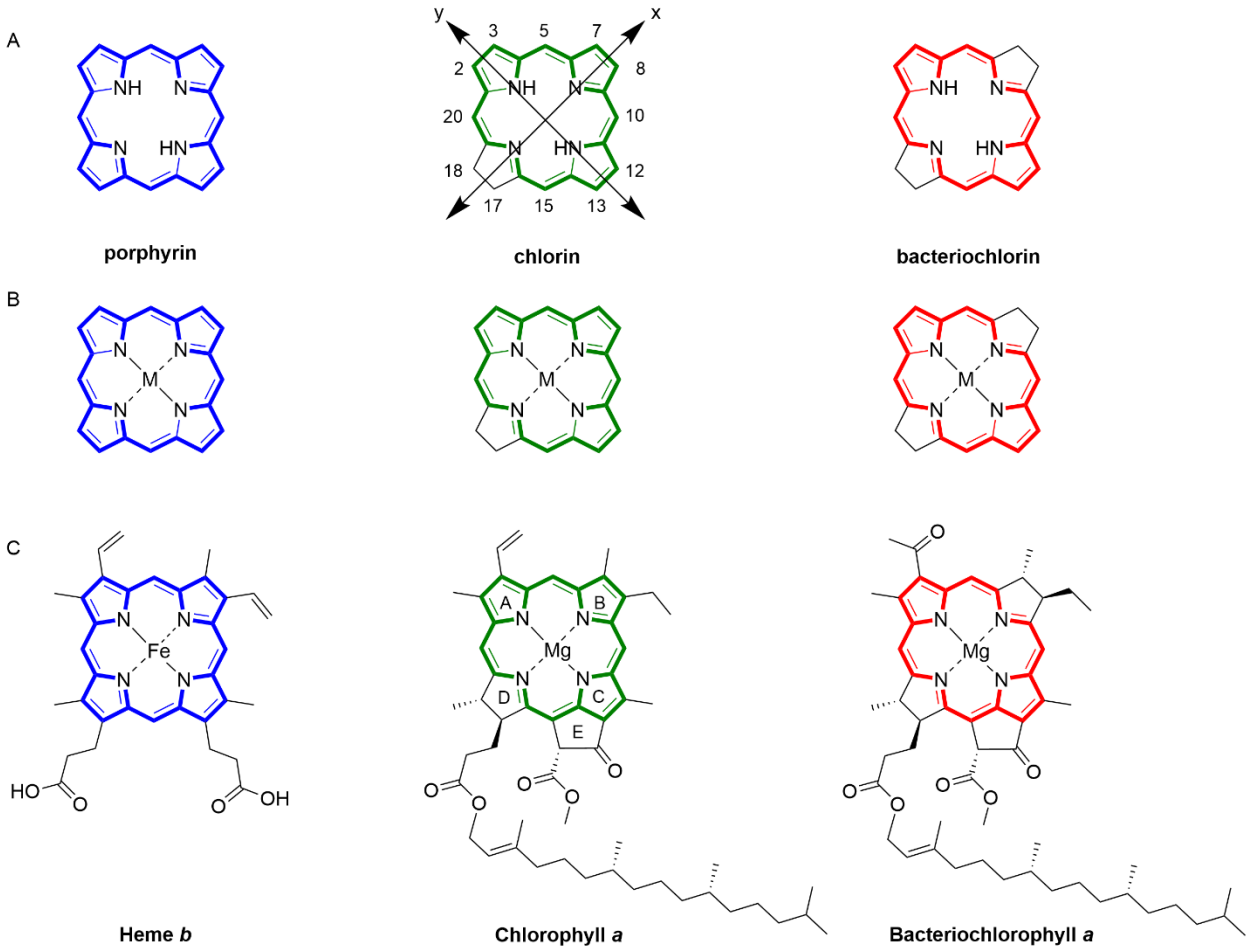


**Fig. 1** Three tetrapyrrole families (porphyrins, chlorins, bacteriochlorins) shown as the metal-free form of parent analogs (A), metal-containing parent analogs (B), and natural members (C). The universal numbering system is shown for the chlorin in (A), indicating the positions that are saturated in progressing from porphyrin to chlorin (17,18) and then to bacteriochlorin (7,8). The standard macrocycle x- and y-axis directions for all the macrocycles are shown for the chlorin in (A).

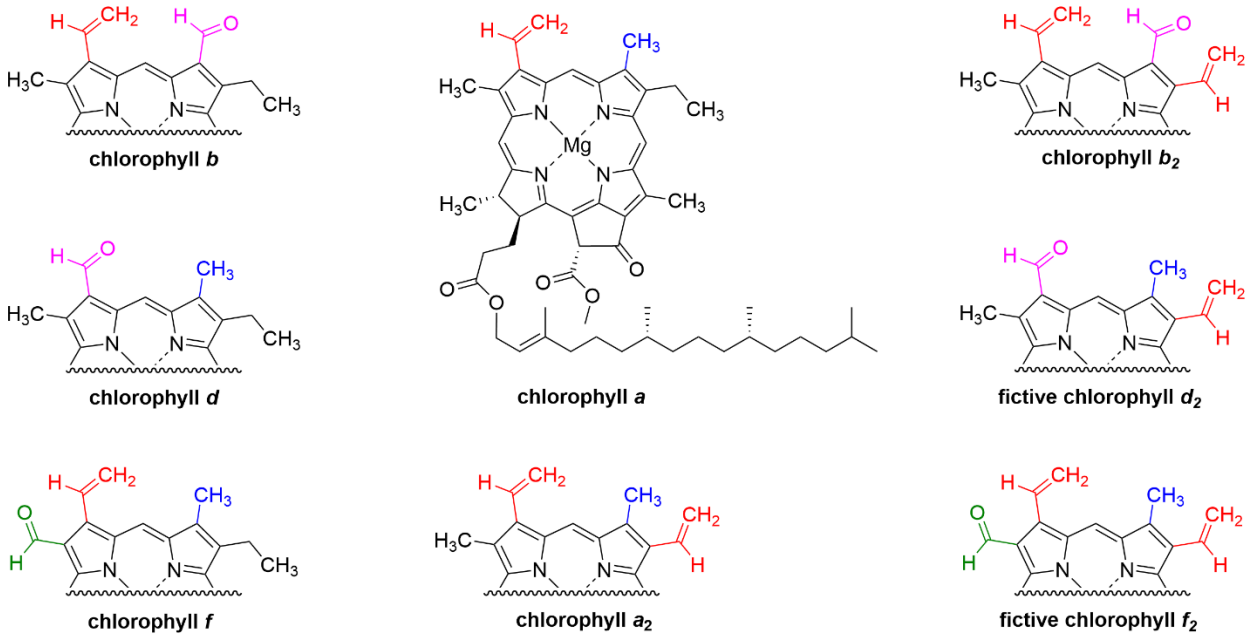


**Fig. 2** Representative chlorophylls. The truncated structures are identical with that of **Chl *a***.

Insight into redox properties of the macrocycles is essential if electron transfer is an integral process or if unwanted electron transfer could impede utility, as in light harvesting or optical imaging, for example. The redox properties of natural chlorophylls (e.g., Chl *a*, Chl *b*, Chl *d*, and Chl *f*) and the metal-free (free base) analogs known as pheophytins (e.g., Ph *a*, Ph *b*, and Ph *d*) have been investigated.[12-14] The redox potentials of bacterial photosynthetic pigments including bacteriochlorophyll *a* (BChl *a*) and bacteriopheophytin *a* (BPh *a*) have been determined.[12,15,16] Such studies provide valuable data but only treat a small subset of the variety of known native macrocycles.[1,17] While the redox properties of synthetic porphyrins have been more studied than for synthetic chlorins and bacteriochlorins,[15,16,18] the redox properties of the vast number of synthetic tetrapyrrole macrocycles understandably have not been measured. The absence of redox data in the majority of cases places reliance on heuristics for estimating changes in redox properties among structurally similar compounds.

Redox properties of a new tetrapyrrole construct are often inferred on the basis of chemical intuition and knowledge of redox potentials of analogs that may differ in substituents and/or macrocycle type (e.g., bacteriochlorin versus chlorin). In this regard, one often has better insight or intuition into relative propensities for oxidation rather than reduction. For example, in the photosynthesis community, it is well understood that chlorophyll *a* is harder to oxidize than bacteriochlorophyll *a*. Similarly, in the tetrapyrrole community, it is general knowledge that a porphyrin is harder to oxidize than the analogous chlorin, which in turn is harder to oxidize than the corresponding bacteriochlorin. However, drawing conclusions on the relative reduction potentials of tetrapyrroles (on the basis of relative oxidation potentials and chemical intuition) often leads to incorrect predictions.

Another point of intuition predicts that the $S_0 \rightarrow S_1$ absorption band should progressively shift to higher energy (shorter wavelength) for the series porphyrin $\rightarrow$ chlorin $\rightarrow$ bacteriochlorin on the basis of the structures shown in Fig. 1. This rationale arises because (1) the size of the "electron box" decreases along this series and (2) the "particle in a (linear or circular) box" model posits that the excited-state energy and electron-box size are inversely related. Although the effective electron-box size does decrease along the series porphyrin $\rightarrow$ chlorin $\rightarrow$ bacteriochlorin, other more dominant factors result in spectral shifts of the long wavelength absorption band in the opposite direction.

The underlying reason that common aspects of chemical intuition often fail for tetrapyrroles is because one cannot simply focus on (variations in) the highest occupied molecular orbital (HOMO) and the lowest unoccupied MO (LUMO). One must also consider variations in the HOMO-1 and LUMO+1. Depending on the structural differences within a set of tetrapyrroles, the energies of the HOMO and LUMO may not track one another. Instead, the HOMO and

LUMO+1 may shift in energy together and the HOMO-1 and LUMO energies may shift in parallel (*vide infra*).

The framework of Gouterman's "four-orbital model"[19-21] explains, as Dr. Gouterman often said, "why grass is green and blood is red." The basis of this model is that absorption of light in the near-ultraviolet to near-infrared regions by porphyrins, chlorins and bacteriochlorins produces excited states that are comprised of linear combinations of configurations derived from one-electron promotions involving the four frontier MOs: HOMO $\rightarrow$ LUMO, HOMO-1 $\rightarrow$ LUMO+1, HOMO $\rightarrow$ LUMO+1, and HOMO-1 $\rightarrow$ LUMO. Mixing of the four one-electron excited-state configurations (configuration interaction) gives rise to the familiar $B_y$, $B_x$, $Q_x$ and $Q_y$ absorption bands. These bands undergo hyperchromic, hypochromic, hypsochromic and/or bathochromic shifts depending on how the macrocycle type (porphyrin, chlorin or bacteriochlorin), metalation state, and substituent pattern affect the relative energies of the four frontier MOs.[19-21]

The focus in the present Perspective is not on optical spectra (and thus *not* on the spacing between MOs, compositions of excited states, and configuration interaction), but on properties that derive directly from the energies of individual orbitals themselves. The intent is to provide deeper insight into the relative redox potentials of related tetrapyrroles. We have encountered these issues in our work over the years when a new tetrapyrrole macrocycle is obtained and its relative ease of oxidation and reduction compared to an analog is sought. These efforts motivated the present Perspective. Examples are provided to underscore the factors at play. Analysis of literature redox data is supported by the results of density functional theory (DFT) calculations. These molecular-orbital (MO) theory calculations are not intended to obtain absolute values of redox potentials. The intent is to understand trends in measured redox potentials and, in case of some of the chlorophylls, how those trends might help gauge redox potentials that have not been measured for some analogs. The rationale is that comparison of MO electron-density distributions and energies

for a set of related tetrapyrroles give physical insight into the origins of relative redox potentials that may not be obvious from the measured values or those calculated *de novo*.

## METHODS

DFT calculations were performed with Gaussian 09 version E.01.[22] Calculations were performed for molecules in toluene using the polarizable continuum model (PCM). Molecular geometries were fully optimized using the hybrid B3LYP functional and 6-31G* basis set. The same geometries are obtained using other functionals (e.g., ωB97XD) and basis sets (e.g., 6-31++G**). Starting with the same optimized geometry, single point calculations of the ground-state molecular orbitals (MOs) were performed using the hybrid B3LYP functional and 6-31G* basis set, while others used the long range corrected ωB97XD functional and 6-31++G** basis set. Calculations that utilized both density functional/basis set combination give the same trends in MO energies. This ensures that conclusions drawn regarding trends in MO energies are independent of the details of the calculations. The MO calculations used Gaussian defaults with the exception of the keyword Int=(grid=ultrafine,Acc2E12). MO images were generated from Gaussian outputs using Chemcraft http://www.chemcraftprog.com).

## RESULTS

The top half (section A) of Table 1 lists the MO energies obtained from DFT calculations performed here for the series of chlorophylls Chl *a*, *b*, *d* and *f* (magnesium chlorins) and the series of companion pheophytins Ph *a*, *b*, *d* and *f* (free base chlorins). Also shown are the redox potentials measured by Kobayashi and coworkers in acetonitrile.[12-14] The redox potentials measured in *N*,*N*-dimethylformamide (DMF) tend to be less positive (or more negative) compared to those obtained in acetonitrile but generally follow the same trends.[12-14]

**Table 1.** MO energies and redox potentials of chlorophylls and pheophytins.[a,b]

| Compound | HOMO-1 (ev) | HOMO (eV) | LUMO (eV) | LUMO+1 (eV) | $E^{ox}$ (V) | $E^{red}$ (V) |
|---|---|---|---|---|---|---|
| *A. Molecules for which redox potential are known* | | | | | | |
| Chl *a* | -6.86 | -6.46 | -1.42 | -0.46 | +0.81 | –1.12 |
| Chl *b* | -7.00 | -6.75 | -1.47 | -1.01 | +0.94 | –1.02 |
| Chl *d* | -6.95 | -6.58 | -1.70 | -0.66 | +0.88 | –0.91 |
| Chl *f* | -6.97 | -6.65 | -1.79 | -0.61 | +0.92 | –0.75 |
| Ph *a* | -7.05 | -6.70 | -1.59 | -0.72 | +1.14 | –0.75 |
| Ph *b* | -7.19 | -6.96 | -1.65 | -1.24 | +1.25 | –0.64 |
| Ph *d* | -7.18 | -6.81 | -1.89 | -0.93 | +1.21 | –0.63 |
| *B. Molecules for which redox potential are estimated here* | | | | | | |
| Chl $a_2$ | -6.89 | -6.52 | -1.46 | -0.62 | 0.85 | -1.06 |
| Chl $b_2$ | -7.03 | -6.76 | -1.51 | -1.13 | 0.95 | -1.02 |
| Chl $d_2$ | -6.99 | -6.62 | -1.72 | -0.83 | 0.90 | -0.84 |
| Chl $f_2$ | -7.01 | -6.70 | -1.81 | -0.78 | 0.93 | -0.77 |
| Ph $a_2$ | -7.10 | -6.74 | -1.63 | -0.88 | 1.17 | -0.70 |
| Ph $b_2$ | -7.23 | -6.98 | -1.68 | -1.36 | 1.26 | -0.68 |
| Ph $d_2$ | -7.22 | -6.86 | -1.91 | -1.08 | 1.22 | -0.61 |
| Ph $f_2$ | -7.24 | -6.93 | -1.99 | -1.02 | 1.24 | -0.59 |
| Ph *f* | -7.20 | -6.89 | -1.97 | -0.86 | 1.23 | -0.60 |

[a]From DFT calculations on molecules in toluene using the ωb97XD functional and 6-31++G** basis set. [b]Redox potentials in section A are the measured values in acetonitrile versus the saturated calomel electrode (SCE).[12-14] Redox potentials in section B are estimated here on the basis of Equations 1–4, which are the equations of the linear fits in Fig. 4A to the measured redox potentials listed in section A .

Fig. 3 gives MO correlation diagrams for the series of chlorophylls Chl *a*, *b*, *d*, and *f* and the series of pheophytins Ph *a*, *b*, *d*, and *f*. Fig. 4A plots the measured[12-14] oxidation and reduction

potential versus the HOMO and LUMO energies for the same series of chlorophylls and pheophytins. The dashed lines are linear fits to the data and are characterized by Equations 1–4.

$$y = -0.842\ x - 2.291 \quad \text{(reduction of chlorophylls)} \tag{1}$$

$$y = -0.230\ x - 1.182 \quad \text{(reduction of pheophytins)} \tag{2}$$

$$y = -0.408\ x - 1.807 \quad \text{(oxidation of chlorophylls)} \tag{3}$$

$$y = -0.414\ x - 1.624 \quad \text{(oxidation of pheophytins)} \tag{4}$$

The lower half (section B) of Table 1 gives calculated MO energies for the chlorophyll and pheophytin $a_2$, $b_2$, $d_2$ and $f_2$ variants as well as for Ph *f*, whose structures are shown in Fig. 2. To our knowledge, the redox potentials for these variants have not been measured. In this regard, Chl $d_2$, Chl $f_2$, Ph $d_2$ and Ph $f_2$, in which a vinyl group is placed at the 8-position, appear not to have been discovered in nature but Chl $a_2$ and Chl $b_2$ are known.[23,24] The MO data were input into Equations 1–4 (describing the dashed lines in Fig. 4A) to estimate (using the calculated MO energies) the redox potentials for the chlorophylls and pheophytins for which such data are currently unavailable. The values are given in the last two columns of the lower half (section B) of Table 1 and are plotted in Fig. 4B (open symbols). Fig. 4B also reproduces the data plotted in Fig. 4A for the chlorophyll and pheophytin variants with measured redox potentials (closed symbols).

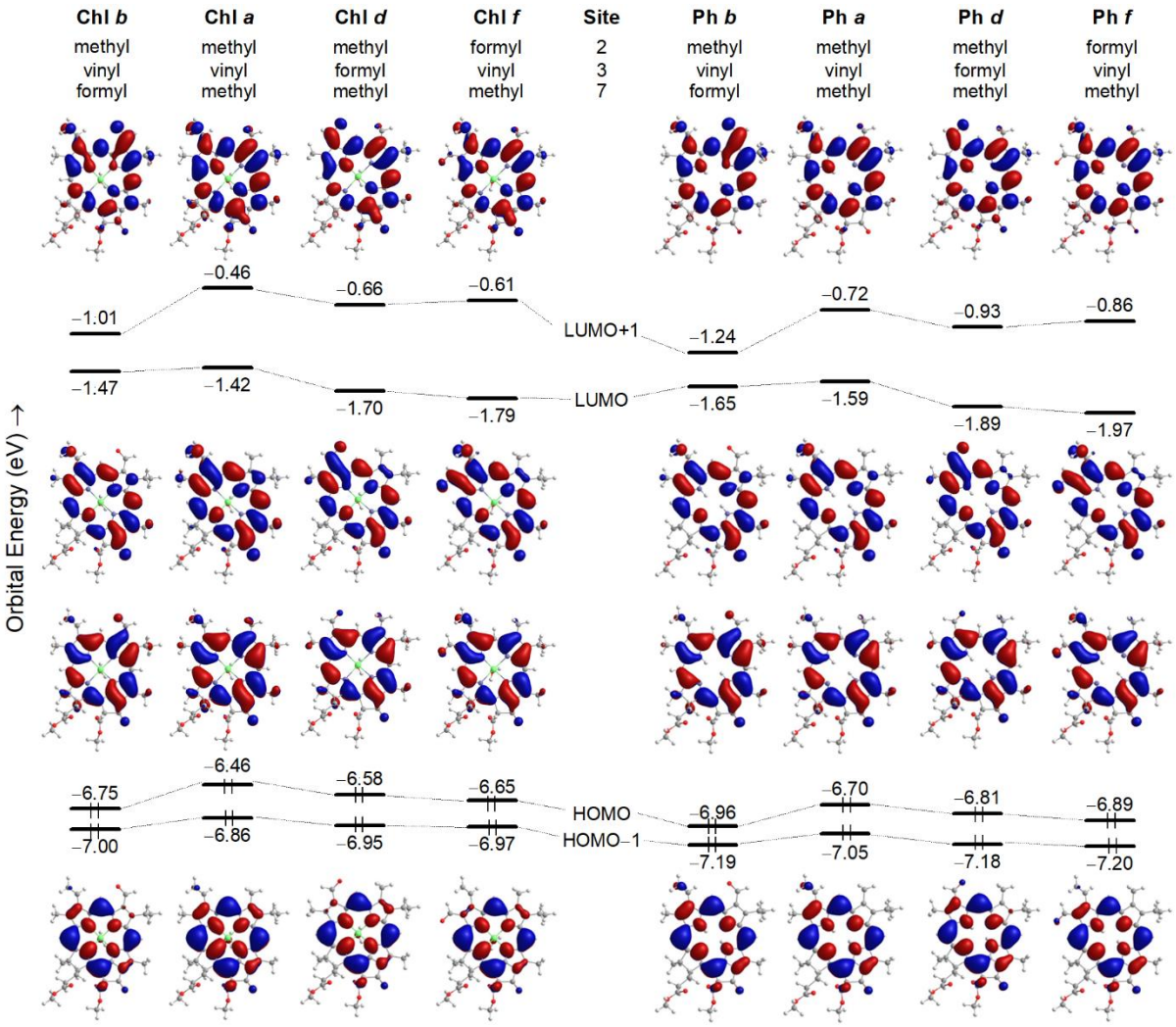


**Fig. 3** MO correlation diagram for the chlorophylls and pheophytins using the data in section A of Table 1. Refer to Fig. 2 for the structures.

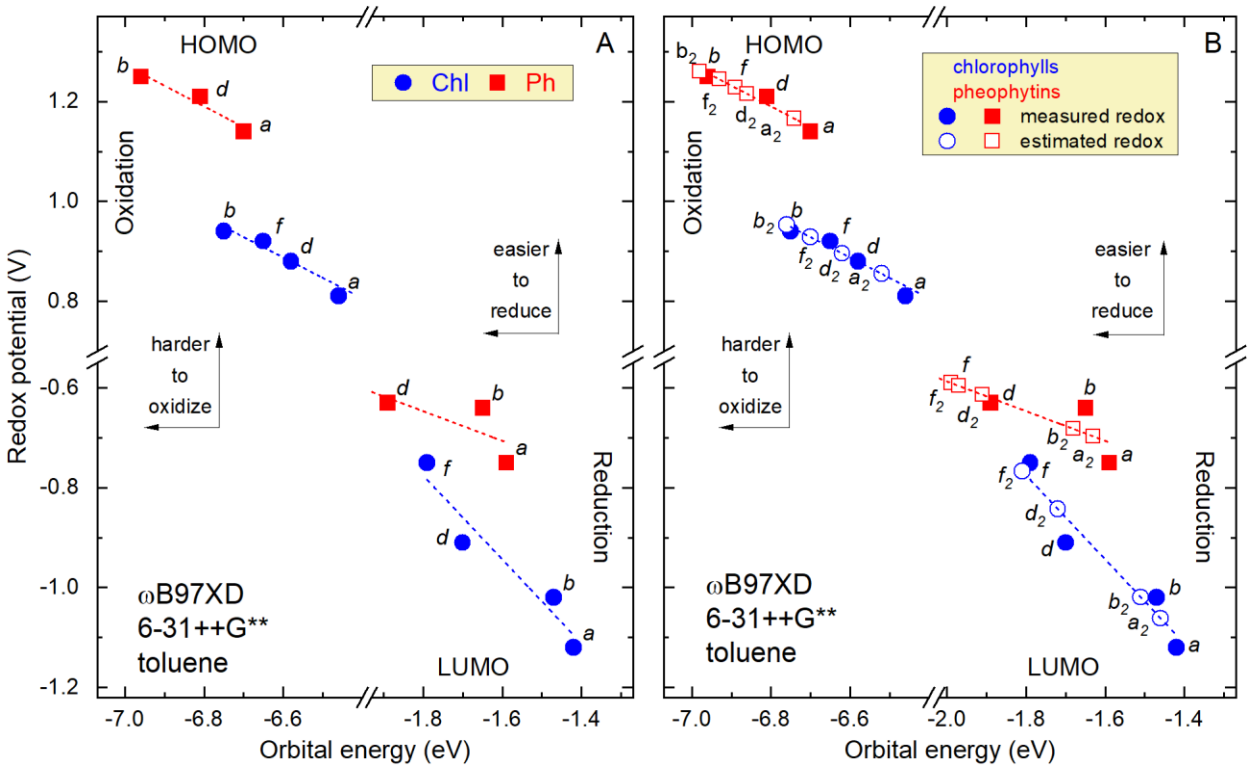


**Fig. 4** (A) Trends in measured redox potential (measured in acetonitrile[12-14]) versus MO energy (obtained employing the ωB97XD functional, 6-31++G** basis set and molecules in toluene) for chlorophylls and pheophytins using the data in the upper half (section A) of Table 1. The linear fits to the data (dashed lines) are described by Equations 1–4. (B) The same information as in panel A (closed symbols and dashed lines) to which is added the redox potentials (open symbols) for chlorophylls and pheophytins that were estimated by inputting the associated MO energies (given in the lower half, section B, of Table 1) into Equations 1–4 (again describing the dashed lines as in panel A).

Table 2 gives literature values for the redox potentials for select porphyrins, chlorins and bacteriochlorins. The list includes several natural photosynthetic pigments, the common synthetic tetrapyrroles *meso*-tetraphenylporphyrin ($H_2$TPP), *meso*-tetraphenylchlorin ($H_2$TPC), *meso*-tetraphenylbacteriochlorin ($H_2$TPBC), 2,3,7,8,12,13,17,18-octaethylporphyrin ($H_2$OEP) and 2,3,7,8,12,13,17,18-octaethylchlorin ($H_2$OEC), and various metal chelates of the common synthetic tetrapyrroles. Table 3 gives the MO energies of the four frontier MOs of the zinc chelates and free base forms of the parent porphyrin (i.e., porphine), chlorin and bacteriochlorin, where

each macrocycle is devoid of peripheral substituents. Fig. 5 gives an MO correlation diagram, and MO electron-density distributions, for the sets of zinc and free base parent tetrapyrroles. The same trends in MO energies among the molecules are obtained using the ωb97XD functional and 6-31++G** basis-set (Table 3 and Fig. 5) and the B3LYP functional and 6-31G* basis set (not shown).

**Table 2.** Redox properties of some tetrapyrroles (versus SCE).[a]

| Compound | $E^{ox}$ | $E^{red}$ |
|---|---|---|
| *Porphyrins* | | |
| MgTPP | +0.54 | –1.35 |
| | +0.72[b] | |
| ZnTPP | +0.71 | –1.35 |
| | +0.86[c] | –1.33[c] |
| $H_2$TPP | +0.95 | –1.05 |
| | +1.08[c] | –1.07[c] |
| MgOEP | +0.54 | –1.68 |
| | +0.43[b] | |
| ZnOEP | +0.63 | –1.61 |
| | +0.52[b] | |
| | +0.67[c] | –1.61[c] |
| $H_2$OEP | +0.81 | –1.46 |
| | +0.90[c] | –1.40[c] |
| *Chlorins* | | |
| ZnTPC | +0.63[c] | –1.33[c] |
| $H_2$TPC | +0.90[c] | –1.12[c] |
| ZnOEC | +0.39[c] | –1.61[c] |
| $H_2$OEC | +0.69[c] | –1.38[c] |
| Chl *a* | +0.52 | –1.12 |
| Ph *a* | +0.86 | –0.93 |

| | | |
|---|---|---|
| *Bacteriochlorins* | | |
| ZnTPBC | +0.18 | |
| $H_2$TPBC | +0.40 | –1.10 |
| BChl *a* | +0.40 | –1.08 |
| | +0.27[d] | |
| BPh *a* | +0.72 | –0.82 |

[a] Oxidations are in butyronitrile or $CH_2Cl_2$ and reductions are in DMF unless noted otherwise.[15] Similar values are known.[16] [b]In DMF.[15] [c]In DMF.[25] [d]In MeOH.[15]

**Table 3.** MO energies and redox potentials of parent porphyrins, chlorins and bacteriochlorin.[a]

| Compound | HOMO-1 (ev) | HOMO (eV) | LUMO (eV) | LUMO+1 (eV) |
|---|---|---|---|---|
| **ZnP** | -6.99 | -6.93 | -1.13 | -1.13 |
| **ZnC** | -7.04 | -6.51 | -1.13 | -0.43 |
| **ZnBC** | -6.97 | -5.90 | -1.32 | +0.47 |
| **$H_2$P** | -7.05 | -7.01 | -1.28 | -1.27 |
| **$H_2$C** | -7.00 | -6.62 | -1.27 | -0.63 |
| **$H_2$BC** | -6.92 | -6.09 | -1.40 | +0.19 |

[a]From DFT calculations on molecules in toluene using the ωb97XD functional and 6-31++G** basis set.

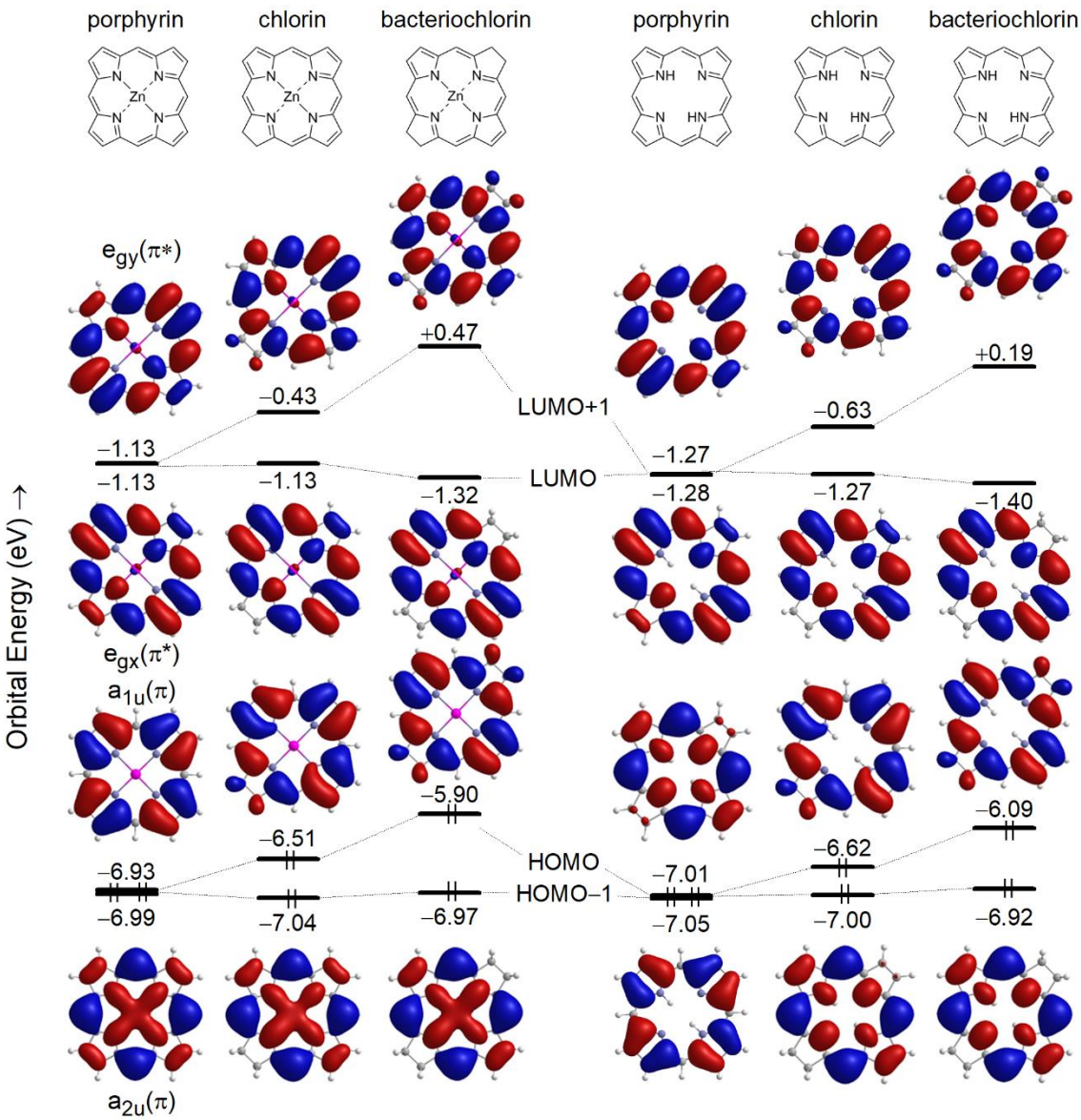


**Fig. 5** MO correlation diagram for zinc chelates (left) and free base forms (right) of the parent porphyrin, chlorin and bacteriochlorin using the MO energies given in section A of Table 3. The calculations employed the ωB97XD functional, 6-31++G** basis set and molecules in toluene.

The parent zinc porphyrin in Fig. 5 (**ZnP**) has $D_{4h}$ symmetry. The LUMO and LUMO+1 are a degenerate pair $e_{gx}(\pi^*)$ and $e_{gy}(\pi^*)$. [The conventional choice of x and y axes and numbering of macrocycle positions is given for the free base chlorin in Fig. 1.] The $e_{gy}(\pi^*)$ orbital places considerable electron density at the 17- and 18-positions; the latter are hydrogenated to produce the corresponding chlorin; which in turn is additionally hydrogenated at the 7,8-positions to give the bacteriochlorin. The $e_{gx}(\pi^*)$ orbital has far less electron density at the 7,8,17,18-positions.

The two highest filled orbitals of **ZnP**, $a_{1u}(\pi)$ and $a_{2u}(\pi)$, are very close in energy and are often referred to as being "accidentally degenerate." Which of these two orbitals is the HOMO for porphyrins depends on the nature, positions and number of substituents on the macrocycle. The HOMO (by a very small amount) for **ZnP** via the DFT calculations performed here is the $a_{1u}(\pi)$ orbital, which has substantial electron density at the 7,8,17,18-positions. The other filled orbital, the $a_{2u}(\pi)$ orbital, has less electron density at these positions but has extensive electron density at the meso-carbons, nitrogens and the central metal ion (if present).

Fig. 6 plots the energies of the four frontier MOs obtained from DFT calculations that "walk" various substituents – methyl (Me), formyl (F), acetyl (A), vinyl (V) – around the perimeter of the zinc chlorin (**ZnC**) macrocycle. We have employed such diagrams previously.[26] The horizontal bars show the energies of the frontier MOs of the corresponding unsubstituted porphyrin (**ZnP**).

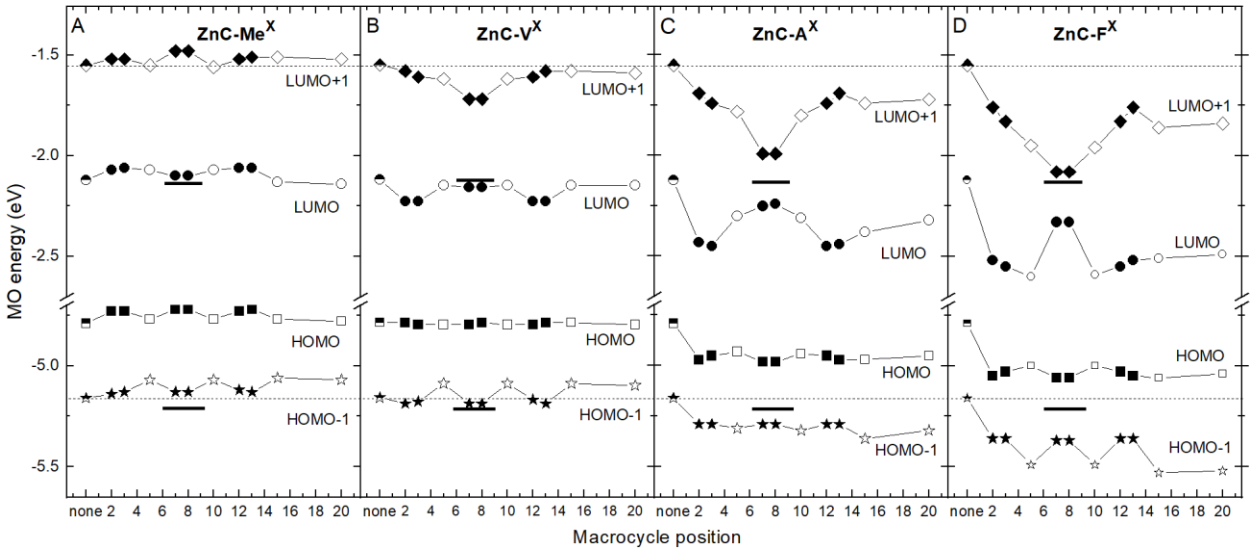


**Fig. 6** Energies of the four frontier MOs obtained from DFT calculations (using the B3LYP functional and 6-31G* basis set) for when walking a methyl (A), vinyl (B), acetyl (C), or formyl (D) group around the **ZnC** macrocycle. The horizontal bars show the energies of the frontier MOs of the corresponding porphyrin (**ZnP**) with no substituents. For **ZnP**, the LUMO and LUMO+1 are rigorously degenerate and the HOMO and HOMO-1 are nearly degenerate.

## DISCUSSION

A long-term objective in chemistry is to acquire foundational knowledge in support of a science of design, where molecules with desired properties can be predicted on the basis of reliable guidelines. Predicting redox properties is essential for any process where electron or hole transfer may ensue. Over the years in working with numerous porphyrins, chlorins, and bacteriochlorins, both native pigments and synthetic analogs, we have come to realize that simple intuition (on the basis of expected inductive or conjugative effects, size of the electron box, etc.) is not entirely reliable in making the types of predictions one wants in development of artificial molecular architectures with target properties. In this section, we first consider the trends in redox potentials and MO energies and follow with in-depth analysis of the effects of free base versus metal chelate, peripheral substituents, and nature of the chromophore (porphyrin, chlorin, bacteriochlorin). The analysis in total provides a deeper understanding of the redox properties of diverse tetrapyrrole macrocycles.

### Trends in redox potentials and MO energies

Fig. 7 relates the ease/difficulty of oxidation or reduction with the redox potential ($E^0$) and MO energy. The figure presents, in a more general manner, the trends indicated in Fig. 4 for chlorophylls and pheophytins. When comparing redox potentials and MO energies for pairs or sets of tetrapyrroles, oxidation becomes harder as the $E^0$ for the first oxidation (often denoted $E^{ox}$) becomes more positive and the HOMO energy becomes more negative. Similarly, the reduction becomes harder as the $E^0$ for the first reduction (often denoted $E^{red}$) becomes more negative and the LUMO energy becomes less negative (or more positive).

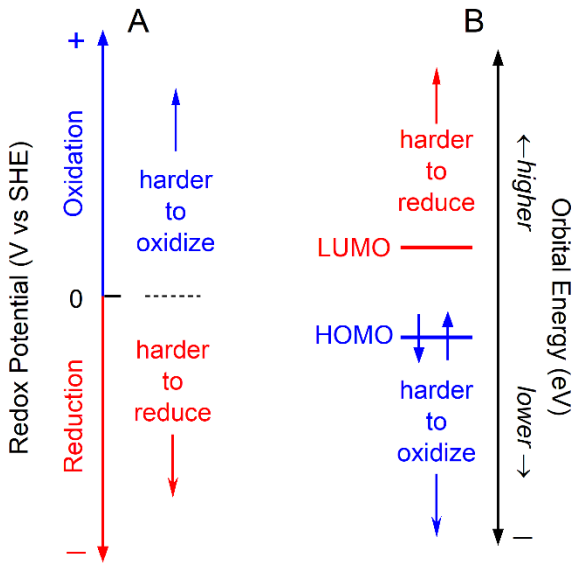


**Fig. 7** The ease/difficulty of oxidation or reduction versus the redox potential (A) and orbital energy (B). The reference redox potential will shift from zero for an electrode different than the SHE. Filled MOs have negative energies. Some (or all) unoccupied MOs may have positive energies depending on the calculation method. Such differences do not change the general trends indicated in the figure.

Redox potentials ($E^0$) are tabulated for half reactions written as reductions. The corresponding process occurs at the electrode, which for the standard hydrogen electrode (SHE) has $E^{ref} = 0$. Thus, the reduction process in Eq. 5B has $E^0$ as tabulated, and the spontaneity of the process (Eq. 6; the Nernst equation) will decrease as the $E^0$ for first reduction ($E^{red}$) becomes more negative ($\Delta G$ becomes less negative or more positive). An actual oxidation process is the reverse of Eq. 5A. Thus, insertion of $E^0$ with the opposite sign of the tabulated value in Eq. 6 indicates that the spontaneity will decrease as the $E^0$ for the first oxidation ($E^{ox}$) becomes more positive.

$$A^+ + e^- \rightarrow A \qquad E^0 = E^{ox} \tag{5A}$$

$$B + e^- \rightarrow B^- \qquad E^0 = E^{red} \tag{5B}$$

$$\Delta G^0 = -n\,F\,E^0 \tag{6}$$

The more negative the orbital energy, the larger the effective attraction (of the molecule) for an electron, corresponding to increased stabilization. In other words, the more negative a filled orbital is in energy, the harder it will be to remove a bound electron (oxidation). The more negative an empty orbital is in energy, the easier it will be to add an electron (reduction).

Figure 8 illustrates changes in MO energies engendered upon making molecular alterations to a reference tetrapyrrole denoted Compound 1. For example, addition of an electron donating group to Compound 1 to attain Compound 2 may shift both the HOMO and LUMO to higher energy (e.g., take on less negative values). The potential for the first oxidation ($E^{ox}$) is expected to track the HOMO energy because an electron is removed from that orbital upon oxidation. Similarly, the potential for the first reduction ($E^{red}$) is expected to track the LUMO energy because that is the orbital into which an electron is added upon reduction. Thus, for the situation depicted in Fig. 8, Compound 2 would be easier to oxidize and harder to reduce than Compound 1. This change arises because destabilization of the HOMO makes it easier to remove an electron from that (filled) orbital and destabilization of the LUMO makes it harder to add an electron to that (empty) orbital.

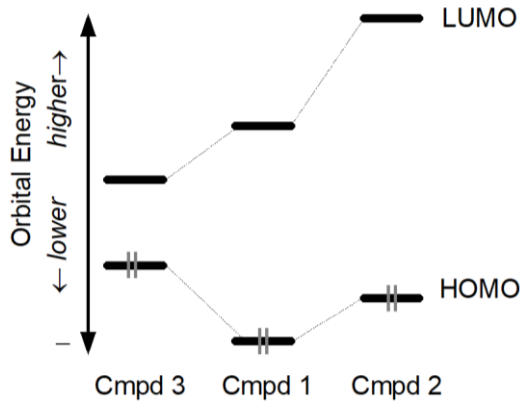


**Fig. 8.** Schematic MO diagram for three related compounds in which the frontier MOs are altered via inductive and/or conjugative effects. Compound 2 is easier to oxidize and harder to reduce than Compound 1. Compound 3 is easier to oxidize and easier to reduce than Compounds 1 and 2.

As a second example, Compound 1 could be altered by addition of a conjugative substituent or an annulated ring to effectively increase the size of the π-electron system to afford Compound 3. One possible result is that the HOMO is destabilized and the LUMO is stabilized, which would also decrease the LUMO–HOMO energy gap. In this case, Compound 3 would be easier to oxidize and easier to reduce than both Compounds 1 and 2. Of course, multiple effects may be at play that influence relative MO energies and redox potentials when altering metalation state, adding macrocycle substituents, or changing macrocycle type for tetrapyrrolic systems. These points are illustrated in the examples given below.

**Comparing the metal chelate and free base form of the same tetrapyrrole**

The oxidation potential for each pheophytin in Table 1 is more positive than for the corresponding chlorophyll. These experimental results are consistent with the relative HOMO energies, where the value for each pheophytin in Table 1 is more negative than for the corresponding chlorophyll. Thus, the free base form (pheophytin) is *harder to oxidize* than the magnesium chelate (chlorophyll). The values in Table 1 show that each pheophytin is in turn *easier to reduce* than its chlorophyll counterpart. The reduction potential for each pheophytin is less negative than for the corresponding chlorophyll. Similarly, the LUMO energy for each pheophytin is more negative than for the corresponding chlorophyll. The simultaneous greater difficulty of oxidation and greater ease of reduction for each pheophytin (free base form) than the corresponding chlorophyll (magnesium chelate) is seen graphically in Fig. 4A. For each point on the plot for a pheophytin (red) the point for the analogous chlorophyll (blue) is lower (less positive $E^{ox}$ and more negative $E^{red}$) and to the right (less negative MO energy).

The data in Table 2 also show that free base forms of porphyrins, chlorins and bacteriochlorins are in general simultaneously harder to oxidize and easier to reduce than their

metal chelates. The zinc chelates are in turn harder to oxidize and easier to reduce than the magnesium chelates. This follows a general trend in electronegativity $Mg^{2+} < Zn^{2+} < 2H^{+}$ and thus the extent to which the electron density from the tetrapyrrole macrocycle is removed by a central metal or protons.[27] [π-Conjugation effects involving the p or d orbitals of metal ions also affect the MO energies.[19-21]]

The trends in redox properties in Table 2 are evidenced by the more positive oxidation potentials paired with the less negative reduction potentials for the free base macrocycles ($H_2$TPP, $H_2$TPC, $H_2$TPBC, $H_2$OEP and $H_2$OEC) versus the corresponding zinc chelates. The comparisons between free base and metal chelate hold even if the redox potentials are not measured in the same solvent, including ones in which solvent molecules likely ligate to the central metal ion. In this regard, solvent molecules that contribute lone-pairs of electrons (e.g., nitrogenous bases) to the central metal via axial ligation would tend to raise certain orbitals in energy, particularly the $a_{2u}(\pi)$-like orbital (which is the HOMO-1 for chlorins and bacteriochlorins and some porphyrins). If the HOMO and LUMO are elevated in energy, the metal chelates would be easier to oxidize and harder to reduce compared to the behavior in the absence of the apical ligand(s). The data in Table 2 show that such effects of axial ligation generally do not overcome the more dominant and opposing effect on MO and redox properties of the two central protons compared to a metal ion.

**Substituent effects on the redox properties and MO energies of chlorophylls and pheophytins**

***Overview.*** The general trends in redox properties of the chlorophylls and pheophytins in Table 1 have been discussed in terms of inductive and conjugative effects of the substituents on the macrocycle.[12-14] Comparisons of Chl *a*, Phe *a*, BChl *a*, and BPh *a* show that oxidation potentials generally trend well with HOMO energies, but reduction potentials exhibit less

correlation with LUMO energies.[12] Here we build on these ideas with the results of additional DFT calculations.

The differences in redox potentials of the various chlorophylls (and pheophytins) derive from the differences in combination of substituents (methyl, vinyl, acetyl, formyl) at the 2,3,7,8-positions (Fig. 2) and their effects on the four frontier MOs (Fig. 3). Fig. 6 aids in sorting out the complex interplay of effects of the different substituents at different positions by walking each of these substituents individually around each position of the **ZnC**, which serves as a simple surrogate for chlorophyll. Similar effects are observed for the magnesium chlorin, free base chlorin and analogs that contain ring E of the natural photosynthetic pigments.[26] Fig. 6 shows that the potency of effects on the frontier MOs increases in the order methyl < vinyl < acetyl < formyl. A given substituent may have much different effects at the 2,3-positions than at the 7,8-positions.

***Comparison of Chl* a, *Chl* d, *and Chl* f *and comparison of Ph* a, *Ph* d, *and Ph* f.** Again, Fig. 4 shows the measured redox potentials of a set of chlorophylls and companion pheophytins[12-14] plotted against the HOMO and LUMO energies obtained from DFT calculations performed here (section A of Table 1). The redox data show that oxidation becomes harder and reduction becomes easier in progressing from Chl *a* to Chl *d* to Chl *f*. The same trend is observed in progressing from Ph *a* to Ph *d* (redox data are not available for Ph *f*). Thus, common chemical intuition (Fig. 8) holds here.

These trends in redox properties can be understood in terms of the effects on the HOMO and LUMO of the individual substituents at specific positions of chlorophyll surrogate **ZnC** in Fig. 6. The impact of the substituents on MO energies generally increases in the following order: 2-methyl (present in Chl *a* and *d*; Fig. 2) < 7-methyl (Chl *a*, *d*, and *f*) < 3-vinyl group (Chl *a* and *f*) << 2- or 3-formyl (Chl *f* or *d*). The combined effects of these groups are evident in the MO correlation diagrams for the chlorophylls and pheophytins (Fig. 3). These substituent effects on

the LUMO and HOMO also provide a basis for understanding the much greater difference in reduction potential than oxidation potential in progressing from Chl *a* to Chl *d* to Chl *f* (Fig. 4A and Table 1).

***Comparison of Chl* b *with Chl* a *and comparison of Ph* b *with Ph* a.** The replacement of the 7-methyl of Chl *a* (and Ph *a*) with the 7-formyl of Chl *b* (and Ph *b*) (Fig. 2) dictates the differences in redox properties of these pigments. Fig. 6A shows the relatively small effects of a methyl group on the energies of the frontier MOs of **ZnC**, which again serves as a proxy for chlorophyll to probe the impact of a given substituent at all possible macrocycle positions. In comparison, Fig. 6D shows that the $e_{gx}$-like LUMO is dramatically elevated in energy (to less negative values) by placing a formyl group at the 7- or 8-positions compared to other sites around the periphery of a chlorin macrocycle. Similarly, the $e_{gy}$-like LUMO+1 is dramatically lowered in energy (to more negative values) by placing a formyl group at the 7- or 8-positions.

The solid bars in Fig. 6 at the 7,8-positions give the MO energies for the corresponding unsubstituted porphyrin (**ZnP**) formed by 7,8-dehydrogenation (oxidation) of **ZnC**. In this regard, recall that the LUMO and LUMO+1 of **ZnP** are rigorously degenerate and that the HOMO and HOMO-1 are "accidentally degenerate." Indeed, a formyl group at the 7- or 8-position tends to "porphyrinize" the chlorin, as we have discussed previously.[26] In other words, the combination of inductive and conjugative effects of a 7- or 8-formyl group tends to reverse the effects of the hydrogenation (reduction) that occurs at those positions on progressing from porphyrin to chlorin.

Overall, Fig. 6 shows that replacement of 7-methyl with 7-formyl (Chl *a* versus Chl *b*; Fig. 2) stabilizes both the HOMO and LUMO, with the larger effect on the LUMO. This makes Chl *b* both harder to oxidize and easier to reduce than Chl *a*. These differences are seen in the redox potentials in Table 1 and Fig. 4A. Fig. 4A also shows that points for Chl *b* and Ph *b* are vertically

above (more positive $E^{ox}$ and less negative $E^{red}$) and to the left (more negative HOMO and LUMO energies) of those for Chl *a* and Ph *a*.

***Comparison of Chl* b *with Chl* d *and Chl* f*, and comparison of Ph* b *with Ph* d *and Ph* f.** The effects on MO energies of walking a given substituent around the periphery of **ZnC** (Fig. 6) show that the potency of substituents increases in the following order: methyl < vinyl < formyl. Additionally, compared to no substituent, a 2- or 3-formyl group stabilizes the LUMO more than the HOMO, yet the reverse is true for a 7-formyl group. The combined impact of the formyl, vinyl, and methyl substituents (Fig. 2) of Chl *b* (2-methyl, 3-vinyl, 7-formyl), Chl *d* (2-methyl, 3-formyl, 7-methyl), and Chl *f* (2-formyl, 3-vinyl, 7-methyl) on the relative MO and redox properties of these three chlorophylls can be seen in Fig. 4A. Chl *b* is both *harder to oxidize and harder to reduce* than Chl *d* and Chl *f*. Similarly, Ph *b* is harder to oxidize and (very slightly) harder to reduce than Phe *d*. Thus, the relative redox potentials of "*b"* versus "*d"* and "*f"* variants of the photosynthetic pigments do not follow the same trend as the "*b*" vs "*a*" analogs described above.

**Comparison of redox properties and MO energies of tetrapyrrole homologs.**

The analysis now turns to comparing the properties of analogs across the three families of tetrapyrrole chromophores, including the natural photosynthetic pigments (Figs. 1 and 2). The conversion of a porphyrin to a chlorin involves $2e^-$, $2H^+$ hydrogenation (typically at the 17,18-positions, ring D) and the subsequent conversion of a chlorin to a bacteriochlorin involves a second $2e^-$, $2H^+$ hydrogenation (typically at the 7,8-positions, ring B). The porphyrin – chlorin – bacteriochlorin set comprises a homologous series with companion effects on electronic structure that include the following. (1) $\pi$-electron delocalization encompasses fewer bonds along the series porphyrin > chlorin > bacteriochlorin. (2) The dehydrogenated 7,8,17,18-positions present increased $\sigma$-electron density to the macrocycle, analogous to an electron-donating substituent.

Both effects tend to progressively destabilize the frontier MOs that have appreciable electron density at the 7,8,17,18-positions.

Relevant here are the results of the MO calculations given in Table 3 and Fig. 5 for the parent porphyrin, chlorin and bacteriochlorin zinc chelates. The $a_{1u}(\pi)$-like filled orbital has substantial electron density at the 7,8,17,18-positions and notably increases in energy along the series. This orbital is the HOMO for essentially all chlorins and bacteriochlorins and some porphyrins (depending on substituents). On the other hand, the $a_{2u}(\pi)$-like filled orbital does not vary greatly in energy across analogous members of the three tetrapyrrole families. This orbital is the HOMO-1 for essentially all chlorins and bacteriochlorins as well as some porphyrins. The LUMO and LUMO+1 for the highly symmetric **ZnP** are a degenerate pair $e_{gx}(\pi^*)$ and $e_{gy}(\pi^*)$. The $e_{gy}(\pi^*)$ orbital places substantial electron density at the 7,8,17,18-positions. This orbital is stabilized along the series porphyrin < chlorin < bacteriochlorin. The $e_{gy}(\pi^*)$ orbital is the LUMO+1 for chlorins and bacteriochlorins. The $e_{gx}(\pi^*)$ orbital, which has little electron density at these sites, changes little in energy along the series. This orbital is the LUMO for chlorins and bacteriochlorins.

The results in Table 3 and Fig. 5 show that in progressing from porphyrin to chlorin to bacteriochlorin, the HOMO (the orbital from which an electron is removed upon oxidation) is progressively destabilized. However, the LUMO does not experience parallel destabilization. Instead, it is the LUMO+1 (which is not involved in reduction) that changes in parallel. The LUMO (the orbital into which an electron goes upon reduction) changes very little, paralleling the HOMO-1 (which is not involved in oxidation).

Thus, Chl *a* is harder to oxidize than BChl *a* by ~120 mV and is also slightly harder to reduce by ~40 mV (Table 1). Ph *a* is harder to oxidize than BPh *a* by ~140 mV and is harder to reduce by ~110 mV. [These plant versus bacterial photosynthetic pigments also differ in the nature

of the 3-substituent.] Synthetic free base chlorin $H_2$TPC is harder to oxidize than synthetic free base bacteriochlorin $H_2$TPBC by ~50 mV and also slightly (~20 mV) harder to reduce. On the basis of the MO results (Table 3 and Fig. 5), one might expect that relative $E^{red}$ values of analogous members of the porphyrin, chlorin and bacteriochlorin families would depend strongly on the medium, which is the protein matrix for photosynthetic pigments and analogs substituted into a cofactor site.

## OUTLOOK

This Perspective provides a framework for understanding trends in redox properties of related pairs or sets of tetrapyrroles. Examples, have been given for tetrapyrroles that differ in metalation state (free base versus metal chelate), substituent effects (depending on the nature and sites of substitution), and macrocycle type (porphyrins versus chlorins versus bacteriochlorins). The framework presented here for assessing trends in redox properties of tetrapyrroles derives from Gouterman's four-orbital model for optical spectra of the same systems. The four-orbital model posits that the optical spectra of tetrapyrroles are described in terms of linear combinations of excited-state configurations derived from one-electron electron promotions from two filled orbitals (HOMO-1 and HOMO) to two empty orbitals (LUMO and LUMO+1).

It is necessarily the case that the first oxidation occurs by removal of an electron from the HOMO and that the first reduction occurs by addition of an electron to the LUMO. However, in assessing how a structural/electronic perturbation (change in metalation state, substituent, or macrocycle type) may affect redox properties, again one cannot simply focus on how the perturbation affects the HOMO and the LUMO but also how it affects the HOMO-1 and LUMO+1. For example, structural perturbations may lead to a greater ease of oxidation along a set of related tetrapyrroles that is understandable in terms of progressive destabilization of the HOMO.

However, the reduction potential may be altered far less because the LUMO energy is relatively unchanged, but instead the LUMO+1 shifts in parallel with the HOMO. In other cases, the energies of the LUMO (involved in reduction) and HOMO-1 (not involved in oxidation) are altered in concert, but the HOMO energy and thus oxidation potential are less perturbed.

Thus, in assessing trends in redox and optical properties of tetrapyrroles, it is important to consider how the energies of all four frontier molecular orbitals are affected. One cannot necessarily predict how the reduction potential of a target tetrapyrrole may differ from that of a reference analog given knowledge of differences in oxidation potential. The rationale is fundamentally connected to the reason that differences in the energy/wavelength of the lowest energy absorption bands of two tetrapyrroles often do not follow expectations inferred from the apparent relative sizes of the π-electron systems. The framework provided here may deepen insights into the functional characteristics of natural photosynthetic systems, aid molecular design in tetrapyrrole science, and provide a richly characterized case in point of a phenomenon of widespread relevance.

**Acknowledgement.** This work was supported by a grant from the Chemical Sciences, Geosciences and Biosciences Division, Office of Basic Energy Sciences, of the U. S. Department of Energy (DE-FG02-05ER15661).

**Conflicts of interest.** There are no conflicts to declare.

**Data availability statement.** The data that support the findings of this study are available within the article.

**Keywords:** photosynthesis, electron-transfer, 4-orbital model, electrochemistry, porphyrin, chlorophyll, bacteriochlorophyll, photochemistry

**Corresponding author contact info:** holten@wustl.edu

## REFERENCES


(1) H. Scheer, In *Chlorophylls and Bacteriochlorophylls. Biochemistry, Biophysics, Functions and Application*, B. Grimm, R. J. Porra, W. Rüdiger and H. Scheer, eds., Springer: Dordrecht, The Netherlands, 2006, pp 1–26.

(2) Y. Chen, G. Li and R. K. Pandey, *Curr. Org. Chem*., 2004, **8**, 1105–1134.

(3) M. A. Grin, A. F. Mironov and A. A. Shtil, *Anti-Cancer Agents Med. Chem*., 2008, **8**, 683–697.

(4) J. S. Lindsey, *Acc. Chem. Res*., 2010, **43**, 300–311.

(5) M. O. Senge, *Chem. Commun.*, 2011, **47**, 1943–1960.

(6) J. S. Lindsey, *Chem. Rev.*, 2015, **115**, 6534–6620.

(7) K. E. Borbas, In *Handbook of Porphyrin Science*, K. M. Kadish, K. M. Smith and R. Guilard, eds., World Scientific Publishing Co. Pte. Ltd.: Singapore, 2016, Vol 36, pp 1–149.

(8) M. Taniguchi and J. S. Lindsey, *Chem. Rev.*, 2017, **117**, 344–535.

(9) C. Brückner, L. Samankumara and J. Ogikubo, In *Handbook of Porphyrin Science*, K. M. Kadish, K. M. Smith and R. Guilard, eds., World Scientific Publishing Co. Pte. Ltd.: Singapore, 2012, Vol 17, pp 1–112.

(10) M. A. Grin and A. F. Mironov, *Russ. Chem. Bull., Int. Ed*., 2016, **65**, 333–349.

(11) S. V. Dudkin, E. A. Makarova and E. A. Lukyanets, *Russ. Chem. Rev.*, 2016, **85**, 700–730.

(12) T. Watanabe and M. Kobayashi, In *Chlorophylls*, H. Scheer, ed., CRC Press: Boca Raton, Florida, 1991, pp 287–315.

(13) M. Kobayashi, S. Ohashi, K. Iwamoto, Y. Shiraiwa, Y. Kato and T. Watanabe, *Biochim. Biophys. Acta*, 2007, **1767**, 596–602.

(14) M. Kobayashi, S. Akutsu, D. Fujinuma, H. Furukawa, H. Komatsu, Y. Hotota, Y. Kato, Y. Kuriowa, T. Watanabe, M. Ohnishi-Kameyama, H. Ono, S. Ohkubo and H. Miyashita, In Chapter 3 https://www.intechopen.com/books/photosynthesis/physicochemical-properties-of-chlorophylls-in-oxygenic-photosynthesis-succession-of-co-factors-from-

(15) R. H. Felton, In *The Porphyrins*, D. Dolphin, ed., Academic Press: New York, 1978, Vol V, pp 53−125.

(16) G. R. Seely, *Photochem. Photobiol.*, 1978, **27**, 639–654.

(17) M. Taniguchi and J. S. Lindsey, *Photochem. Photobiol.*, 2021, **97**, 136–165.

(18) K. M. Kadish, G. Royal, E. V. Caemelbecke and L. Gueletti, In *The Porphyrin Handbook*, K. M. Kadish, K. M. Smith and R. Guilard, eds., Academic Press: San Diego, 2000, Vol 9, pp 1–219.

(19) M. Gouterman, *J. Chem. Phys.*, 1959, **30**, 1139–1161.

(20) M. Gouterman, *J. Mol. Spectroscopy*, 1961, **6**, 138–163.

(21) M. Gouterman, In *The Porphyrins*, D. Dolphin, ed., Academic Press: New York, 1978, Vol 3, pp 1–165.

(22) M. J. Frisch, G. W. Trucks, H. B. Schlegel, G. E. Scuseria, M. A. Robb, J. R. Cheeseman, G. Scalmani, V. Barone, B. Mennucci, G. A. Petersson, H. Nakatsuji, M. Caricato, X. Li, H. P. Hratchian, A. F. Izmaylov, J. Bloino, G. Zheng, J. L. Sonnenberg, M. Hada, M. Ehara, K. Toyota, R. Fukuda, J. Hasegawa, M. Ishida, T. Nakajima, Y. Honda, O. Kitao, H. Nakai,

T. Vreven, J. A. Montgomery Jr., J. E. Peralta, F. Ogliaro, M. Bearpark, J. J. Heyd, E. Brothers, K. N. Kudin, V. N. Staroverov, R. Kobayashi, J. Normand, K. Raghavachari, A. Rendell, J. C. Burant, S. S. Iyengar, J. Tomasi, M. Cossi, N. Rega, J. M. Millam, M. Klene, J. E. Knox, J. B. Cross, V. Bakken, C. Adamo, J. Jaramillo, R. Gomperts, R. E. Stratmann, O. Yazyev, A. J. Austin, R. Cammi, C. Pomelli, J. W. Ochterski, R. L. Martin, K. Morokuma, V. G. Zakrzewski, G. A. Voth, P. Salvador, J. J. Dannenberg, S. Dapprich, A. D. Daniels, Ö. Farkas, J. B. Foresman, J. V. Ortiz, J. Cioslowski and D. J. Fox, *Gaussian 09, version D.01*, Gaussian, Inc., Wallingford CT, 2009.

(23) R. Goericke and D. J. Repeta, *Mar. Ecol. Prog. Ser.*, 1993, **101**, 307–313.

(24) M. Kobayashi, M. Akiyama, H. Kise and T. Watanabe, In *Chlorophylls and Bacteriochlorophylls: Biochemistry, Biophysics, Functions and Applications*, B. Grimm, R. J. Porra, W. Rüdiger and H. Scheer, eds., Springer: Dordrecht, The Netherlands, 2006, pp 55–66.

(25) S. H. Strauss and R. G. Thompson, *J. Inorg. Biochem.*, 1986, **27**, 173–177.

(26) J. W. Springer, K. M. Faries, J. R. Diers, C. Muthiah, O. Mass, H. L. Kee, C. Kirmaier, J. S. Lindsey, D. F. Bocian and D. Holten, *Photochem. Photobiol.*, 2012, **88**, 651–674.

(27) J.-H. Fuhrhop and D. Mauzerall, *J. Am. Chem. Soc.*, 1969, **91**, 4174–4181.